Synthesis of equivalent sources for tyre/road noise simulation and analysis of the vehicle influence on sound propagation

Luca Rapino [a],[*], Francesco Ripamonti [a], Samanta Dallasta [a], Simone Baro [b], Roberto Corradi [a]

[a] Department of Mechanical Engineering, Politecnico di Milano, Via La Masa 1, Milano 20156, Italy
[b] Pirelli Tyre S.p.A., Viale Piero e Alberto Pirelli 25, Milano 20126, Italy

ARTICLE INFO

ABSTRACT

Road traffic noise affects the well-being of people living in urban areas. Amongst the noise sources, tyre/road interaction plays a major role. In this context, predictive acoustic models can be useful for the tyre industry to design quiter tyres. This paper deals with a methodology for simulating tyre/road noise through equivalent monopoles, synthesised using an inverse problem approach, starting from indoor tests performed in a semi-anechoic chamber. A drum with an ISO 10844 road replica is used to obtain realistic tread pattern and road roughness excitations. The experimental setup and a dedicated signal processing technique are described here. To perform the source synthesis, data is combined with acoustic finite element models based on a deformed treaded tyre geometry, in order to take the acoustic resonances at the tyre/road interface into account. The synthesised monopoles are then used to run a numerical simulation including a vehicle in order to consider its influence on sound propagation. The results are then validated by comparing them with indoor measurements.

1. Introduction

Tyre noise is the main contributor to road traffic noise [1,2]. For this reason, regulations have been issued to promote the development of quieter tyres [3–7]. Moreover, interest in tyre/road noise (TRN) has increased in recent decades due to the introduction of electric and hybrid powertrains. These considerations can be generalised by stating that tyre noise is a key performance index for new tyres. However, optimising tyre noise is not a trivial task, as other performance indexes (dry and wet handling, wear, rolling resistance, etc.) may have contrary design requirements. In this context, tyre/road noise predictive models may be beneficial to the automotive industry when it comes to optimising the design of new tyres, improving know-how and defining new acoustic-oriented technical solutions.

In literature, tyre/road noise models are categorised into statistical, deterministic and hybrid models [8]. Statistical models are based on the correlation between measured noise and related tyre/road parameters. Being data-driven, a processing strategy for evaluating the most correlated features is often required [9–11]. Deterministic models are based on knowledge of the physical phenomena and use analytical formulations or numerical techniques, such as the finite element method or the boundary element method [12,13]. Deterministic models are useful for improving an understanding of the mechanisms that generate and amplify tyre/road noise, whereas statistical models provide no physical interpretation of the results.

In terms of the physical mechanisms involved, tyre/road noise is caused by several generation and amplification phenomena [14–17]. On the one hand, generation mechanisms can be classified as vibroacoustic (tread impact, road roughness excitation, running deflection, stick/slip, etc.) and aeroacoustic mechanisms (air turbulence and air pumping). On the other hand, tyre/road noise amplification mechanisms are related to the acoustic resonances in the footprint region, i.e., pipe resonances, horn effect and Helmholtz resonances [18,19]. Generation and amplification mechanisms are strictly related to tyre design parameters. In particular, the tread pattern plays a relevant role, as it is both a generator, due to the tread impact mechanisms, and an amplifier, due to the pipe resonances [20,21].

Some of the deterministic models described in literature focus on modelling tyre/road noise using equivalent sources. This approach is based on solving an inverse problem, as described in [22–24]. In [25], a simulation of sound radiation due to a vibrating tyre surface is compared with the noise radiated by two monopoles in close proximity to a simplified tyre geometry. This analysis highlights the importance of considering the monopoles' phase shift and a distribution of several

---

* Corresponding author.
E-mail address: luca.rapino@polimi.it (L. Rapino).

monopoles to improve the predictions. In [26], a 2D analytical approach based on a multipole model was developed; in this case, the 3D sound field is not modelled, limiting the possibility of predicting the sound levels during pass-by and coast-by noise tests. In [27], a substitution monopole approach was used to predict sound quality indicators. Several monopoles, each characterised by a volume velocity and a phase shift, were used. On testing various source synthesis approaches, the authors observed that there should be at least twice as many microphones as there are monopoles in the model, to obtain reliable results. A contribution to this research field was also made by some of the authors of this paper. In [28], a source synthesis approach based on indoor measurements is described. A dedicated separation algorithm to extract the tread pattern noise is presented and source synthesis based on a set of monopoles radiating in a free field hemi-space is used.

Experimental measurements are fundamental for solving inverse problems. In principle, outdoor or indoor techniques could be adopted. However, outdoor tests are influenced by environmental factors, with a negative impact on test repeatability [29,30], or they require complex experimental setups, like the one described in [31]. For this reason, indoor tests in a semi-anechoic chamber are preferred. Indoor tests also make it possible to perform additional analyses that may support the definition of models. In this context, sound mapping techniques can be used to assess which part of the tyre surface is the main contributor to the radiated sound and, therefore, to evaluate the position of the equivalent sources. In [32], results of planar near field holography and beamforming techniques show that the footprint inlet, outlet and side are the main contributors to generation of the tyre/road noise. In the same reference, the complexity of the sound field is also shown by means of directivity diagrams.

In this context, this paper proposes an approach for synthesising equivalent sources that combines indoor measurements and numerical models. Measurements are processed to separate the tread pattern and the road roughness noise components and to exclude other signal components related to random phenomena, the investigation of which is beyond the scope of this work. Separation of the tread pattern noise and the random component is also described in [28]; in this reference, the road roughness component was not identified since a very smooth road surface was used during the tests. However, in this work, an ISO 10844 road replica was used and the road roughness noise had similar amplitudes to the tread pattern noise. For this reason, a new source synthesis based on identifying both tread pattern and road roughness noise components is described. Furthermore, an acoustic model based on a deformed treaded tyre geometry was used and resonances at the footprint region (i.e., pipe resonances and horn effect) were included, in order to perform a physically-consistent identification of the equivalent sources. In other publications, analytical sound propagation models or numerical models based on simplified tyre geometries, such as slick tyres, were used. Finally, in this work the equivalent sources were used to perform acoustic simulations of tyres fitted on a vehicle. The aim of this analysis is to test the possibility of performing simulations that include a vehicle by using the synthesised sources evaluated from the tests with the tyre only. To validate the results and analyse the car body's influence on sound propagation, indoor tests were also carried out with tyres fitted on a vehicle.

This paper is organised as follows. In Section 2, the indoor test procedure and the data processing done to separate the tread pattern and the road roughness noise components are described. Section 3 deals with the source synthesis methodology, focusing on defining the equivalent sources and the sound radiation model, as well as solving the inverse problem and comparing the results against indoor tests with tyres only. In Section 4, the vehicle's influence on sound propagation is discussed and numerical simulations with a vehicle are validated. Section 5 draws the conclusions from this activity.

2. Indoor tests and separation of noise components

In this work, equivalent sources are synthesised by solving an inverse problem that relies on tyre/road noise measurements. In this section, the execution of the indoor test and the data post-processing are discussed.

2.1. Indoor tests

Tests were performed in Pirelli's semi-anechoic chamber located in Breuberg, Germany. A drum covered with an ISO 10844 road replica was used to obtain tread impact and road roughness excitations coherent with a coast-by outdoor condition. A 225/55 R17 tyre with a tread pattern specifically designed for research purposes was used. It is composed of five ribs, each made up of equally spaced rectangular tread blocks. The tyre was inflated to 2.4 bars and a vertical load of 450 kg was imposed. A constant speed of 80 km/h was selected for carrying out the measurements, in accordance with coast-by conditions. A trigger was used to acquire the time instants of tyre and drum revolutions. Two different microphone arrays were used. The first was a semi-circular array, composed of six microphones located at a height of 0,3 m above the ground, placed at a radial distance of 1,5 m from the footprint centre and separated by 30° angles. These microphones were in the far-field region for frequencies higher than 400 Hz. The second set of receivers was an 8 m linear array composed of seventeen microphones, placed at a distance of 2,2 m from the tyre footprint and at a height of 0,48 m above the ground. The dimensions of this array were a 40 % fraction of those prescribed by the ISO 362–3 standard for the indoor pass-by test [7], and were defined to fit the semi-anechoic room's dimensions. The experimental setup is shown in Fig. 1. A picture of the tyre mounted on the test rig is also provided in Fig. 2a.

Indoor tests were also performed on a vehicle, keeping all the other parameters coherent with the test-rig measurements. A BMW i3 was chosen as the test vehicle. During these tests, the vehicle was turned off, the transmission system removed and the brakes released. Due to the facility's layout, for each test only one tyre was driven by the drum. For this reason, two tests were performed to acquire the noise generated by the front right tyre and then the rear right tyre. This additional set of experimental measurements was not used for source synthesis, but for validation purposes and to investigate the vehicle's influence on sound propagation (see Section 4). A picture of the experimental setup with the vehicle is provided in Fig. 2b.

2.2. Separation of the tyre/road noise components

During constant speed tests, microphone signals have components that repeat every tyre and drum revolution. The periodic component with tyre revolution is related to the tread impact phenomenon as well as tyre non-uniformity, whereas the drum revolution periodicity is associated with the roughness excitation due to the road replica shells applied to the drum. It is worth observing that, despite being a random stationary process in outdoor conditions, road roughness excitation becomes a deterministic phenomenon during indoor tests. Due to the importance of these two periods, in this work each drum and tyre revolution were identified using triggers.

To extract the deterministic part of the signals, the combined period of a complete set of n tyre and m drum revolutions, with n and m being integers, is identified. For the test case discussed in this paper, $n = 99$ and $m = 32$ revolutions were considered, for a combined period of approximately 9,2 s. From these values it can be found that the period of a tyre and a drum revolution are $T_{tyre} = 0.093s$ and $T_{drum} = 0.2875s$, therefore the fundamental frequencies and the frequency resolution of these periodic signal components are approximately $f_{tyre} = 10.8Hz$ and $f_{drum} = 3.5Hz$. These values depend only on the tyre and drum RPMs, for this reason they are specific of considered tyre rolling speed, tyre radius and drum radius. The knowledge of the drum and tyre revolution periods made it possible to convert the signal in the frequency domain and
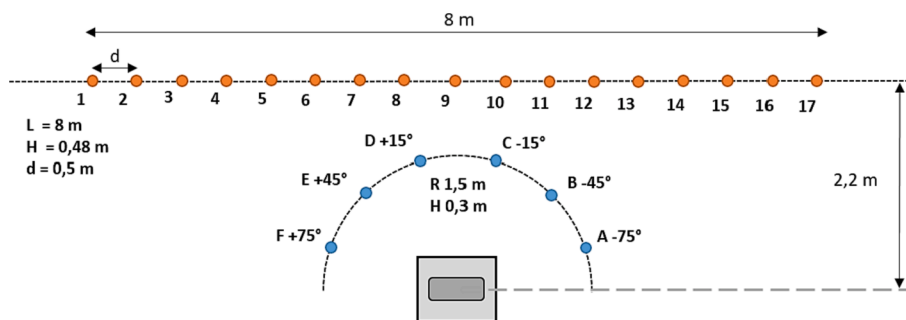
Fig. 1. Top view of the indoor experimental setup with the tyre on the drum. The same microphone configuration was used for the test rig and vehicle tests.
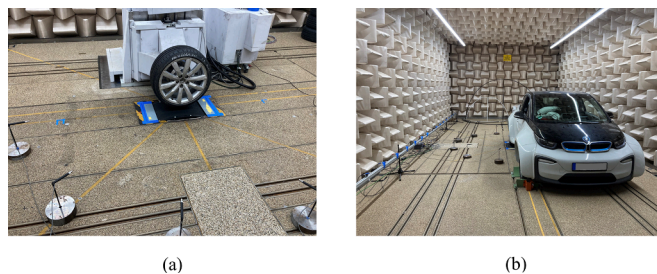

(a)   (b)

Fig. 2. Indoor tests setup. In (a), tests performed on the test rig; the drum was covered with an ISO 10844 road replica. In (b), tests on vehicle; the linear and the semi-circular microphone arrays can be seen.

to select the spectral lines related to the tyre and drum harmonics. Since the time domain signal was cut considering the period of simultaneous completion of n tyre and m drum revolutions, shared harmonics were also present. In this case, it was assumed that the tread impact has the highest contribution to the radiated noise and the signal was only associated with the tread pattern noise. The remaining part of the signal was related to other components (mainly of a random nature) and leakage due to rolling speed fluctuations within the time window processed. In Fig. 3, the result of this separation algorithm is provided. The spectrum of microphone C is represented in grey, whereas red, blue and green markers highlight the spectrum components related to drum, tyre and shared harmonics respectively. The same representation shows also a detail of the spectrum in the 1000–1200 Hz range. It is clearly visible that both drum and tyre harmonics are the highest contributors to the total noise. Harmonics related to both drum and tyre periodicity are also present, whereas all other spectral lines are associated with the effects of other phenomena. It is worth recalling that a higher number of drum harmonics is justified by the fact that the drum radius is approximately three times bigger than the tyre radius. Thus, the drum period is longer and the frequency resolution of drum harmonics is higher than that of the tyre.

Once all the microphones' signals were separated into components, A-weighted Sound Pressure Levels (SPL) ranging from 500 Hz to 2500 Hz one-third octave bands were computed and integrated in an overall A-weighted SPL (OASPL). This metric is relevant for tyre noise applications since pass-by and coast-by tests target this noise level. The aim of this paper is to provide an approach to synthetise equivalent sources to simulate the OASPL related to deterministic phenomena, considering the receivers shown in Fig. 1. Other components, which are mainly related to random phenomena, are disregarded since a deterministic modelling approach like the one discussed in this paper is not suitable for simulating them. By combining tyre and drum harmonics, the deterministic signal component is obtained. In Fig. 4, the OASPLs of the total signal and its components are represented at the microphones' locations. The black line represents the deterministic signal components considered in the sections of this paper that follow.

3. Source synthesis methodology

In order to perform the source synthesis, the layout of the monopoles should be defined and a model for describing the propagation of sound is required. Then, the quantification of the amplitudes and phases (complex source strengths) of the monopoles is performed applying a dedicated inverse problem resolution approach. These topics are discussed in this section.

3.1. Definition of the equivalent monopoles and numerical modelling of the radiated sound

To support the definition of the equivalent monopoles, previous experimental results were considered. Sound mapping activities carried out using beamforming and acoustic holography techniques (see [32]) proved that tyre/road noise is mainly generated at the tyre's footprint, especially at the inlet, outlet and side region. Other experimental tests, the results of which are presented in [28], show the complexity of the sound field radiated by a rolling tyre, as its directivity pattern also depends on the radial distance from the tyre footprint.

These experimental activities, as well as additional results by other researchers (refer to Section 1), led to the definition of a set of equivalent sources made up of nine monopoles (more than two receivers for each source are guaranteed), each characterised by an amplitude and a phase shift to be identified during the source synthesis procedure. Monopoles were placed at the footprint's outlet, inlet and lateral region, and were located in positions at different distances from the tyre footprint. However, the coordinates of monopoles are currently based on user experience, while criteria for deriving their location will be a topic of follow-up research.

In terms of the numerical model used to estimate the sound radiation due to each monopole activation, an acoustic finite element model was defined. This model was based on a treaded tyre geometry that represents the deformation that the system undergoes due to rolling at 80 km/h on a rigid drum (with the same dimensions as that used during the indoor tests). To this end, a specific time instant of a rolling tyre structural simulation was extracted. To obtain a closed tyre surface, the unmodelled wheel rim was replaced by two circular surfaces (see Fig. 5). All the air/structure interfaces were assumed to be acoustically rigid and no dissipation was included as a boundary condition (such as sound absorption acting on surfaces). Since the model was based on a deflected tyre geometry, acoustic amplifications were included in the sound radiation model by properly describing the horn geometry as well as the air volumes inside the tyre grooves. The simulation results were evaluated in terms of sound pressure levels at locations coherent with the positions of the indoor test microphones (see Fig. 1). From an operating point of view, the sound radiation model provided a set of frequency response functions (FRFs) used to relate each monopole to the receivers' signals. The FRFs were simulated via multiple load cases, each referring to a single monopole activation.
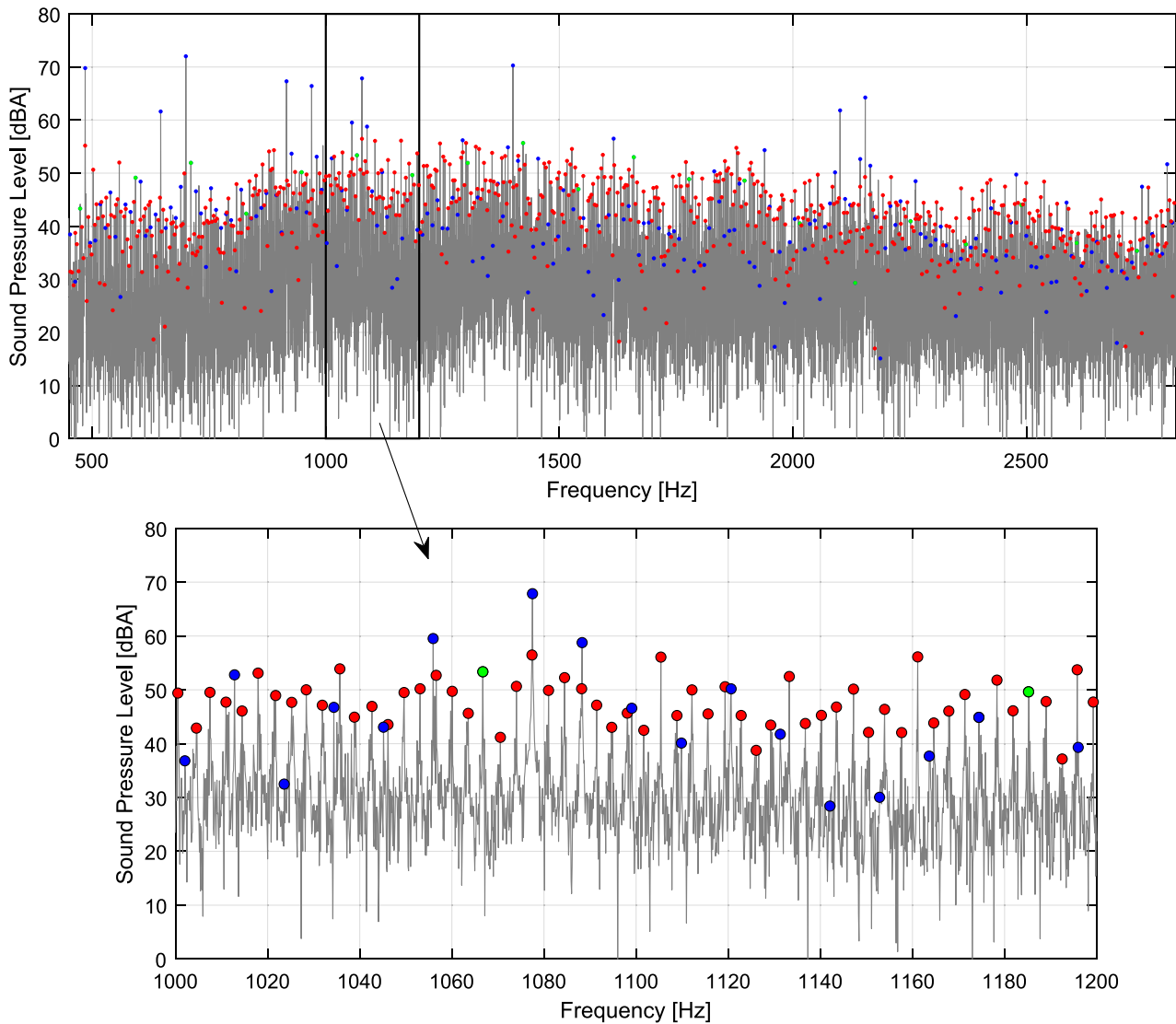
Fig. 3. Graphic representation of the separation of the noise components. In grey, the entire spectrum of the indoor measurement. Peaks related to drum harmonics are highlighted with red dots; in blue, tyre harmonics peaks; in green, peaks related to both drum and tyre periodicity; other signal components are associated with other physical effects. On the bottom, a detail of the upper graph in the 1000 Hz − 1200 Hz frequency range.

3.2. Inverse problem and quantification of the monopoles' source strengths

An inverse problem has to be solved to find the monopoles' source strengths. A dedicated approach is proposed for tackling some specific aspects of the signals measured during this activity.

The core of the inversion procedure is the traditional least-square minimisation of the error $\varepsilon(\omega)$ between the simulated and measured pressures. Given the FRFs matrix $H(\omega)$, the measured pressure vector $p(\omega)$ and the source strengths vector $q(\omega)$, the least-square cost function to be minimised is defined as:

$$\min_{q \in \mathbb{C}^n} J = \frac{1}{2}\varepsilon^H\varepsilon = \frac{1}{2}(Hq - p)^H(Hq - p) \tag{1}$$

where frequency dependency is dropped from the notation since the problem is to be solved at each narrowband frequency. By involving a quadratic cost function, this mathematical optimisation problem only allows a global solution, which is:

$$q = H^+ p \tag{2}$$

where H^+ denotes the pseudo-inverse of the FRFs matrix.

It is worth pointing out that this formulation makes it possible to identify source strengths capable of minimising the error between simulations and measurements in terms of the spectra's real and imaginary parts simultaneously. This can be shown by writing $J = \frac{1}{2}\varepsilon^H\varepsilon = \frac{1}{2}(\varepsilon_{Re}^2 + \varepsilon_{Im}^2)$.

During the indoor tests considered in this work, microphones were placed in positions at distances ranging from 1,5 m to 4,5 m approximately from the tyre footprint. Considering the inverse square law, differences of up to 9.5 dBA are expected in the signals acquired. According to the traditional approach, this can lead to a source synthesis based mainly on signals with higher sound pressure levels, while penalising those with lower levels. To avoid this effect, each microphone signal (made of a real and an imaginary part) is normalised in relation to its amplitude. Thus, the related errors to be minimised are also normalised accordingly, and no penalisation effect is introduced. To this end, a weighting diagonal matrix $W(\omega)$ in which $w_{ii}(\omega) = \frac{1}{\|p_i(\omega)\|}$ is applied to the optimisation problem (where the $\|.\|$ operator indicates the Euclidean L^2 norm). Considering $p_w = Wp$ and $H_w = WH$, Equation (1) can be rewritten as:
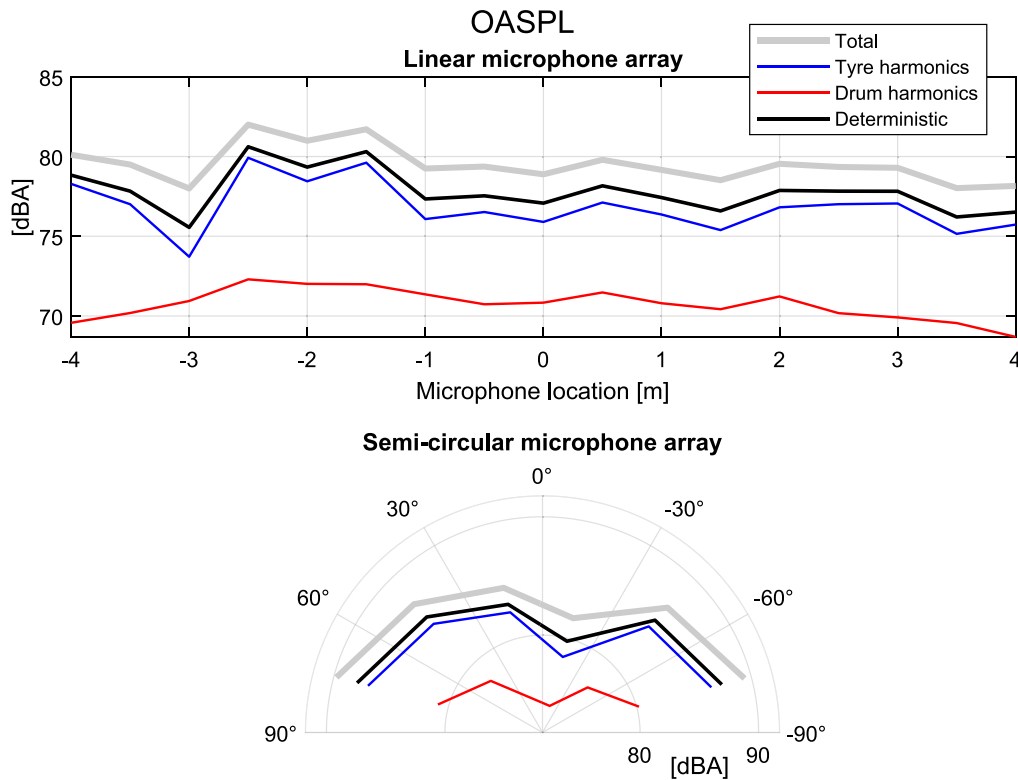
Fig. 4. Overall A-weighted Sound Pressure Levels (OASPL) at linear and semi-circular microphone array locations. The black line is the sum of the tyre and drum harmonics, being the two deterministic components identified from the total signal.
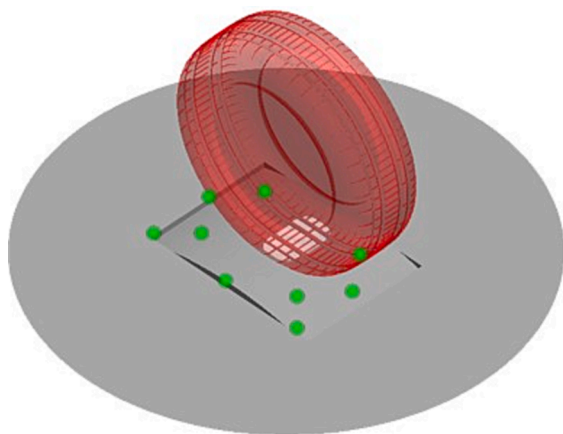

Fig. 5. Numerical model for the evaluation of the acoustic FRFs due to each monopole (green spheres) activation. In transparent red, the deformed tyre on drum (grey). Air volumes inside the grooves at the footprint region are visible.

$$\min_{\boldsymbol{q} \in \mathbb{C}^n} J = \frac{1}{2} \boldsymbol{\varepsilon}_w^H \boldsymbol{\varepsilon}_w = \frac{1}{2} (H_w \boldsymbol{q} - \boldsymbol{p}_w)^H (H_w \boldsymbol{q} - \boldsymbol{p}_w) \tag{3}$$

the solution of which is:

$$\boldsymbol{q} = H_w^+ \boldsymbol{p}_w \tag{4}$$

This problem can find source strengths that optimise the simulated spectra of each microphone, in terms of real and imaginary parts. For this application, reproducing the sound intensity averaged overall the microphones' locations is fundamental. This condition should be added to the optimisation problem as a constraint. This leads to the introduction of a scalar gain factor $\alpha(\omega)$ equal to the ratio between the measured average sound intensity $\|\boldsymbol{p}\|$ and the simulated intensity $\|H\boldsymbol{q}\|$. Finally,

Equation (4) can be re-written as:

$$q = \frac{\|\boldsymbol{p}\|}{\|HH_w^+ \boldsymbol{p}_w\|} H_w^+ \boldsymbol{p}_w \tag{5}$$

Equation (5) involves a pseudo-inverse operator. Thus, regularisation was applied to avoid ill-conditioned problem resolutions (refer to [22,23]). The Truncated Singular Value Decomposition (TSVD) approach was used, considering the first k singular values, which provided a cumulated contribution of at least the 95 % of the original FRFs' signals. The remaining singular values were discarded to avoid ill-conditioned source synthesis. Fig. 6 shows the condition number $\kappa(H_w)$ of the H_w matrix before and after the TSVD regularisation was applied, indicating a clear improvement.

Once the microphones' signals were processed to extract the spectra of the deterministic noise components $\boldsymbol{p}(\omega)$ (Section 2.2) and the FRF matrix $H(\omega)$ was evaluated using the finite element simulation described in Section 3.1, the monopoles' source strengths $\boldsymbol{q}(\omega)$ were obtained by solving the inverse problem. The results were used to evaluate the simulated microphones' spectra $\boldsymbol{p}_s(\omega) = H(\omega)\boldsymbol{q}(\omega)$ and to assess the performance of the source synthesis by a comparison with the original spectra $\boldsymbol{p}(\omega)$. In Fig. 7, an example of the comparison at the C microphone (at -15°) of the semi-circular array (refer to Fig. 1) is shown. The results demonstrates that the proposed approach is capable of simulating the original spectrum with a fair level of accuracy. It is worth mentioning that the sharp tonal peaks visible on both measured and simulated signals are related to the contribution of the tread pattern excitation. For example, the peak visible at approximately 1080 Hz is related to a tread pattern geometrical feature that is repeated 100 times for each tyre revolution. Considering that the tyre revolution frequency was estimated to be approximately 10.8 Hz, a clear relationship between the tread pattern drawing and noise radiation is demonstrated. A correlation between other tread pattern geometrical periodicities and noise peaks is confirmed by iterating the analysis.

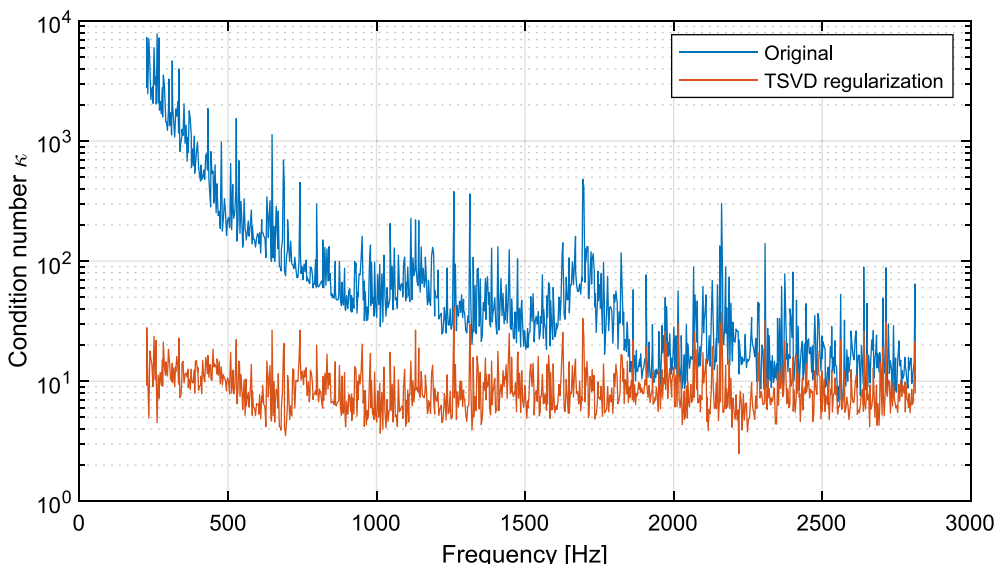A validation in terms OASPL trend across microphone locations was

Fig. 6. Trend of the H_w matrix condition number $\kappa(H_w)$ before and after the TSVD regularisation.
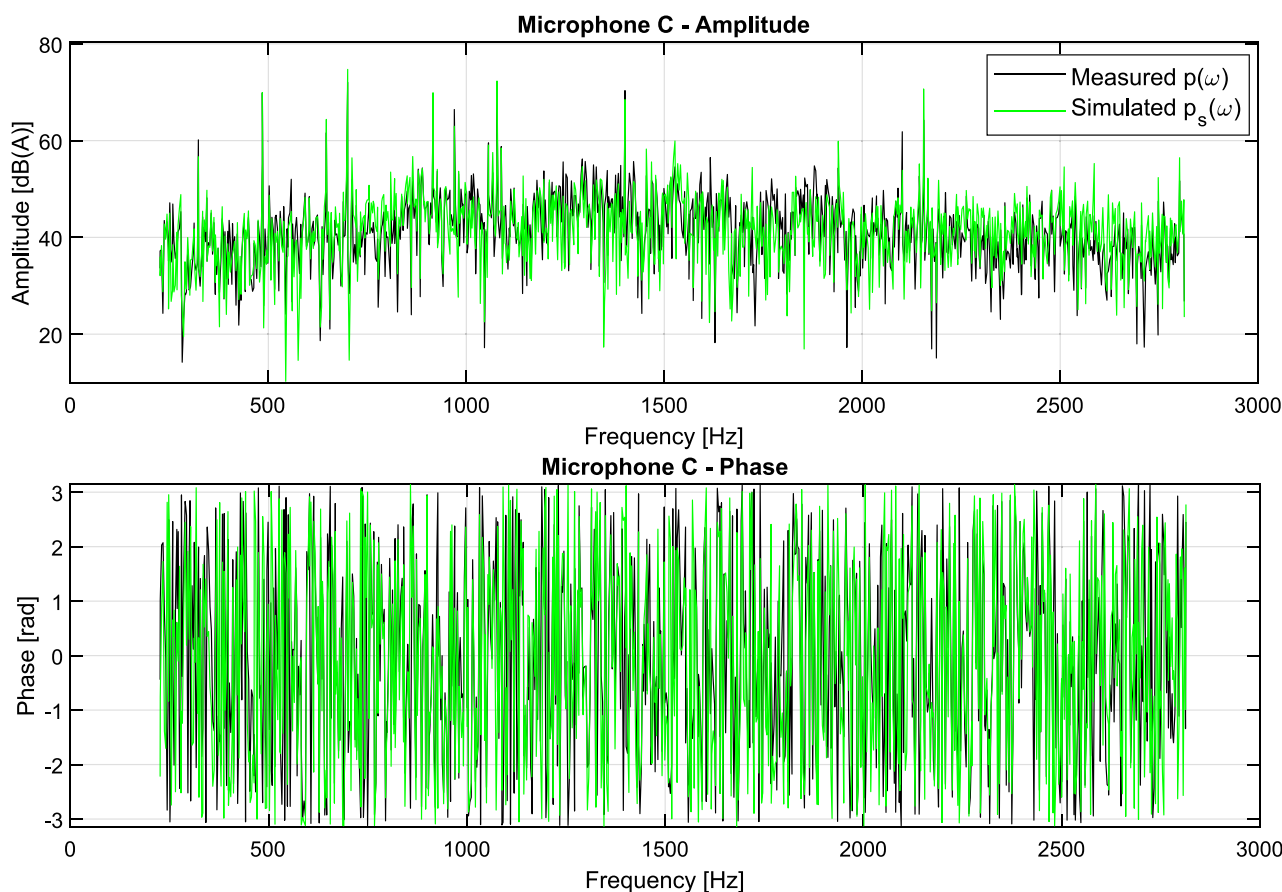

Fig. 7. Comparison of the measured deterministic noise component (in black) against the simulated spectrum (in green) at microphone C (refer to Fig. 1).

also carried out. Results are reported in Fig. 8. In this representation, the black curve refers to the deterministic signal components measured during the indoor tests, in green the simulation result obtained with the proposed methodology, in red dashed lines an additional simulation result to compare the green curve against the standard pseudo-inverse approach described by Eq. (2) and [22,23,27], which does not apply any weighting operation during the source synthesis. The simulation results approximate the general trend of the sound field, even though there are localised under/overestimations. Focusing on the approach proposed in this paper, the green curves seem more in accordance with the experimental result than the standard approach, even though there is a gap at the inlet region (75° and −4 m microphones). It is worth highlighting that the experimental measurements confirm the relevant difference between the maximum (88 dBA at MIC F) and the minimum
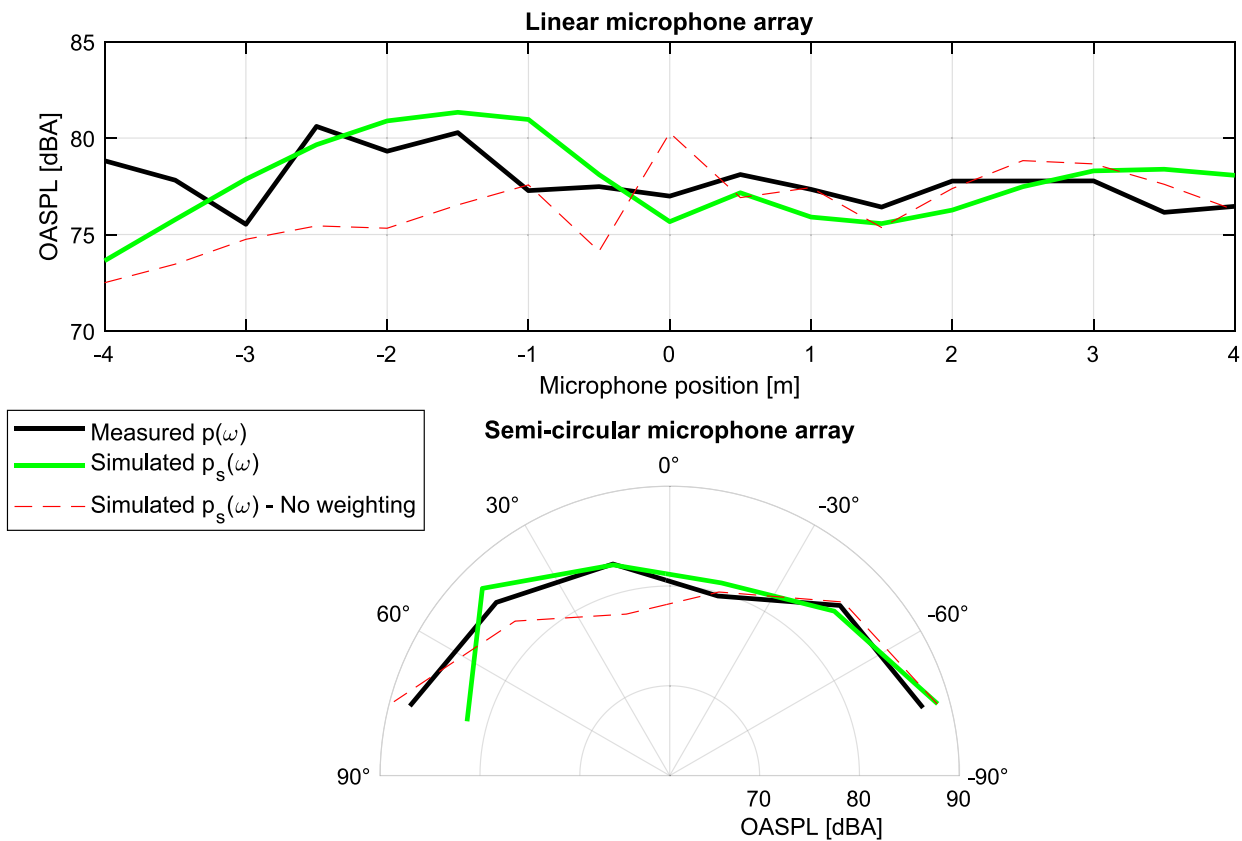
Fig. 8. Comparison of OASPLs between the measured deterministic noise component (in black) and the simulation results (in green). Moreover, a simulation based on monopoles synthetized without applying the weighting matrix (refer to Eq. (2) and [22,23,27]) is shown with dashed red lines.

sound pressure levels (75.5 dBA at MIC 3) of 12.5 dB, justifying the normalisation done during the source synthesis procedure. Additional monopoles could have benefitted this comparison, by making it possible to better match signals that proved to be critical, such as the 75° and −4 m microphones. The results of this practical solution are not reported in this paper, which aims to describe the general procedure and show the potential of the proposed strategy.

4. Acoustic simulation with a vehicle

This work investigates the possibility of performing tyre/road noise simulations of tyres fitted on a vehicle using monopoles evaluated starting from indoor tests carried out without a vehicle. This approach might be useful for tyre makers because indoor tests with vehicle require specific facilities and additional efforts with respect to tests performed with a turret only. Moreover, it may happen that the vehicle to be tested is not available yet and only a virtual prototype could be used. To better explain the approach, a flowchart is represented in Fig. 9. The

equivalent monopoles are synthesized using data that refer to tests and simulations without a vehicle, whereas the simulation with vehicle is based on the same sound sources and updated numerical FRFs. To conclude the study, a validation against experimental measurements performed with a vehicle has been carried out.

To evaluate the numerical FRFs that consider the presence of a vehicle, a new simulation must be defined and a description of a vehicle is required. During this activity, following a reverse engineering approach, the geometry of a BMW i3 was digitalised using a Hexagon Absolute Arm 85 Series equipped with an AS1 laser scanner. This procedure produced a mesh that was coherent with the test vehicle. From an acoustic point of view, the surfaces were assumed to be purely reflective since no acoustic characterisation of the vehicle's components was performed in the framework of this activity. The vehicle's geometry was then included in the acoustic model, also adding the four tyres. It is worth mentioning that the same tyre deformed geometry considered for the source synthesis procedure was used, since the tyres underwent the same vertical loading during the turret and vehicle tests. Since the
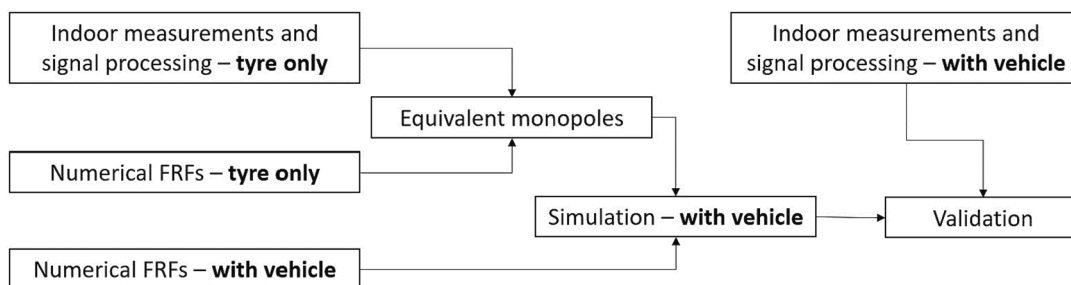

Fig. 9. Flowchart of the approach used to perform an acoustic simulation with a vehicle and to validate the results. Equivalent monopoles are synthetised from indoor measurements performed without a vehicle.

acoustic model was based on a finite element solver, an air volume mesh had to be defined. This was accomplished using an adaptive meshing approach, so that wavelength-dependent (and thus frequency-dependent) meshing requirements were imposed, in order to keep a reasonable number of degrees of freedom in the model. To complete the air volume definition, the free-field condition was included by means of a perfectly matched layer (PML).

Then, equivalent sources and receivers were defined. To be coherent with the indoor tests, the aim of these simulations was to predict the sound field generated by the front right and the rear right tyres rolling independently. For this reason, equivalent monopoles were distributed according to the layout used during the indoor tests of both tyres. Then, two separate load cases were defined in order to simulate each tyre activation independently. Simulated receivers were also duplicated in order to place microphones in the correct position in relation to both tyres. The simulation setup is shown in Fig. 10, with the front and the rear tyre and related receivers highlighted in red and blue respectively.

Once the simulation setup was completed, the same monopoles' source strength evaluated on tyre only were considered to predict the sound field generated by the vehicle-mounted tyres. These results were post-processed to evaluate the OASPL over the frequency range of interest 450–2820 Hz and to validate the same against indoor measurements. It is worth mentioning that, in this section, measurements refer to the indoor tests performed with vehicle (described in Section 1). In this case too, experimental signals were processed to evaluate the tread pattern and the road roughness noise contribution, but this time the signals were not used to perform any source synthesis but were only used to validate the simulations. In Figs. 11 and 12, the front and the rear tyre simulation results (in green) are compared with the experimental measurements (in black). The experimental curves show that the vehicle modified the sound field compared to the turret tests (compare with Fig. 8), with a non-identical effect for the front and rear tyre setups. This is justified by the different wheel arc geometry of front and rear axles. By comparing the simulation results with the experimental measurements, one can see that the quality of the prediction for both the rear and front tyre cases is similar to the simulation without a vehicle (refer to Fig. 8). In particular, the general sound field trend resembles that found experimentally, even though underestimation of the inlet region is seen for the two cases as in the previous validation without a vehicle. Moreover, for the front tyre case, the OASPL peak visible in the experimental measurements at −1,5 m is shifted towards the centre of the array in the numerical result.

5. Conclusions

This paper describes an approach to synthesise equivalent sources used to simulate the tyre/road noise due to a treaded tyre rolling on a rough surface and to investigate the possibility of performing tyre/road noise simulations including the vehicle's influence on sound propagation. This is accomplished by combining indoor measurements taken on drum and acoustic numerical models. A data processing strategy was applied to separate the tread pattern and the road roughness noise components from the measured signals in order to exclude other signal components related to random phenomena. Moreover, a numerical sound radiation model based on a deformed treaded tyre geometry was used to identify the equivalent sources. Finally, the synthesised sources were used for numerical simulations with a vehicle, in order to evaluate the possibility of predicting the sound field of a vehicle-mounted tyre starting from indoor tests performed on the tyre only. To this end, the trend of the OASPL across two microphone arrays was investigated. The simulation results approximate the general trend of the sound field, even though there are localised under/overestimations.

Further development of the current equivalent source model in terms of possible alternatives to the choice of the number and position of the monopoles might be pursued, in order to improve the accuracy of the prediction especially in the high frequency range. Moreover, refinement of the methodology would benefit from additional tests aimed at extending the number of cases included in the source synthesis and validation process, as well as including tyres with different tread patterns. In the project follow-up, the proposed equivalent source model is intended to be finally employed to perform simulations of the outdoor coast-by test.

CRediT authorship contribution statement

Luca Rapino: Conceptualization, Methodology, Investigation, Validation, Writing – original draft. **Francesco Ripamonti:** Conceptualization, Supervision, Writing – review & editing. **Samanta Dallasta:** Investigation, Validation, Writing – original draft. **Simone Baro:** Conceptualization, Supervision, Writing – review & editing. **Roberto Corradi:** Conceptualization, Supervision, Project administration, Writing – review & editing.
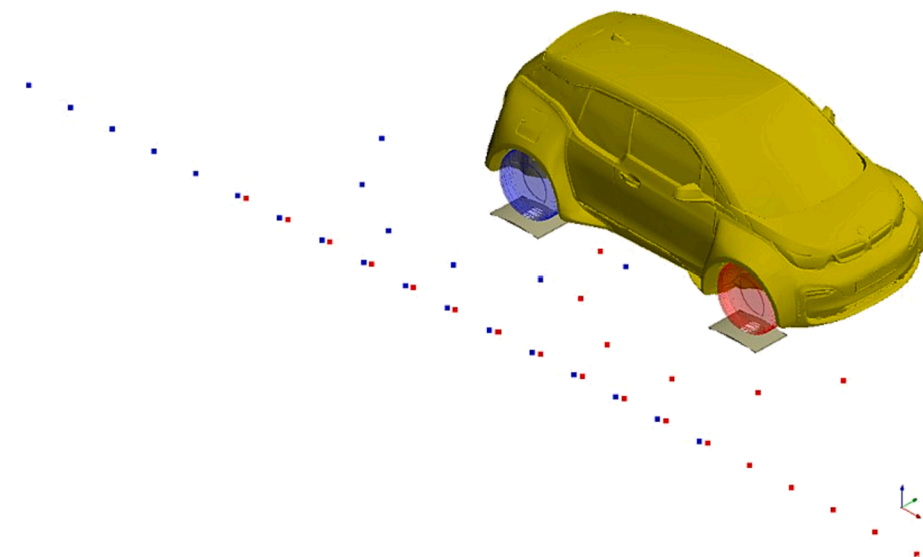
Fig. 10. Acoustic model based on the scanned geometry of the BMW i3 used during the indoor tests. Simulations were carried out with two independent load cases. The receivers related to the front right tyre are shown in red and those for the rear right tyres are in blue.
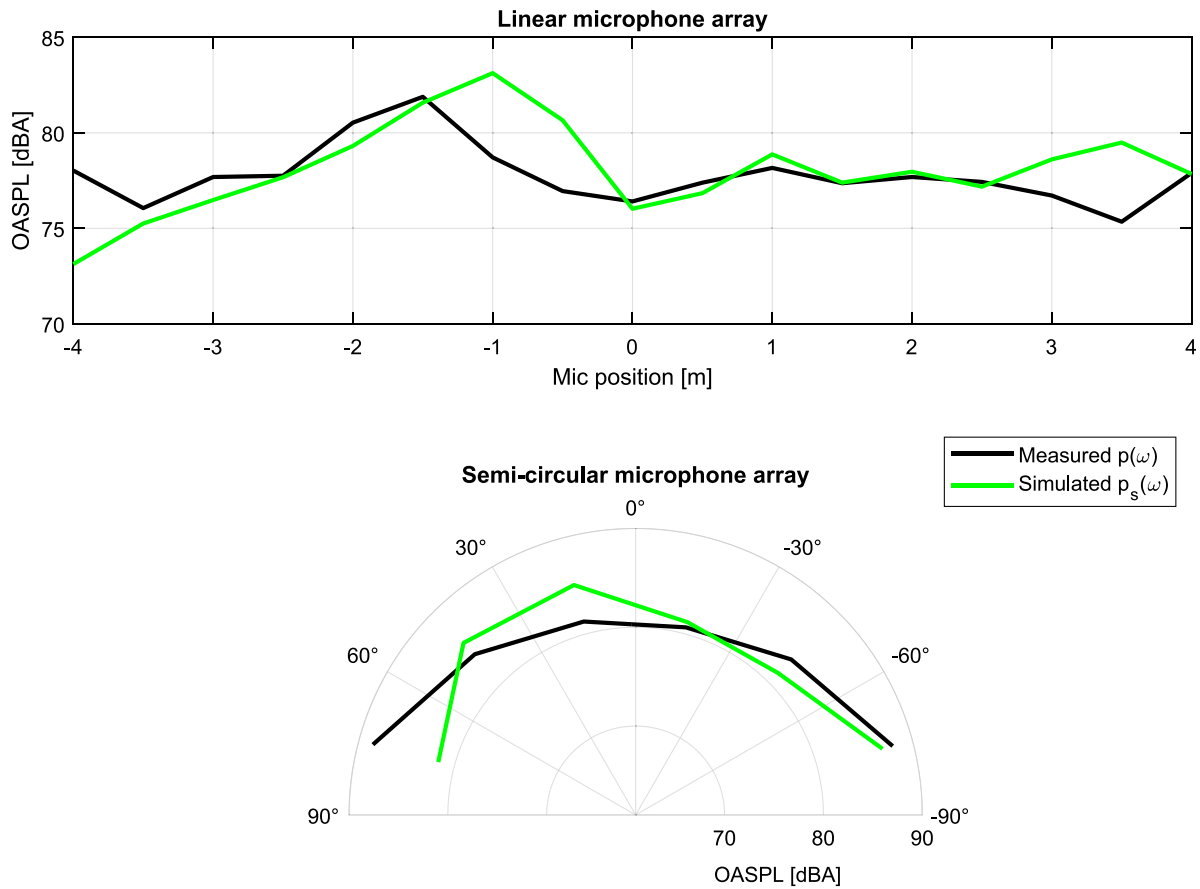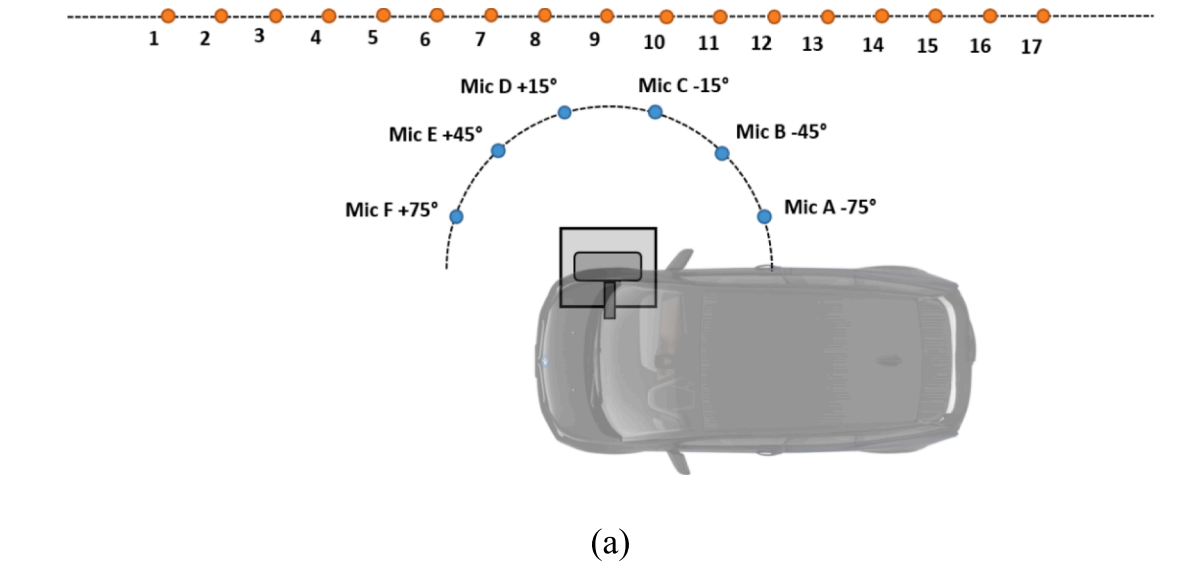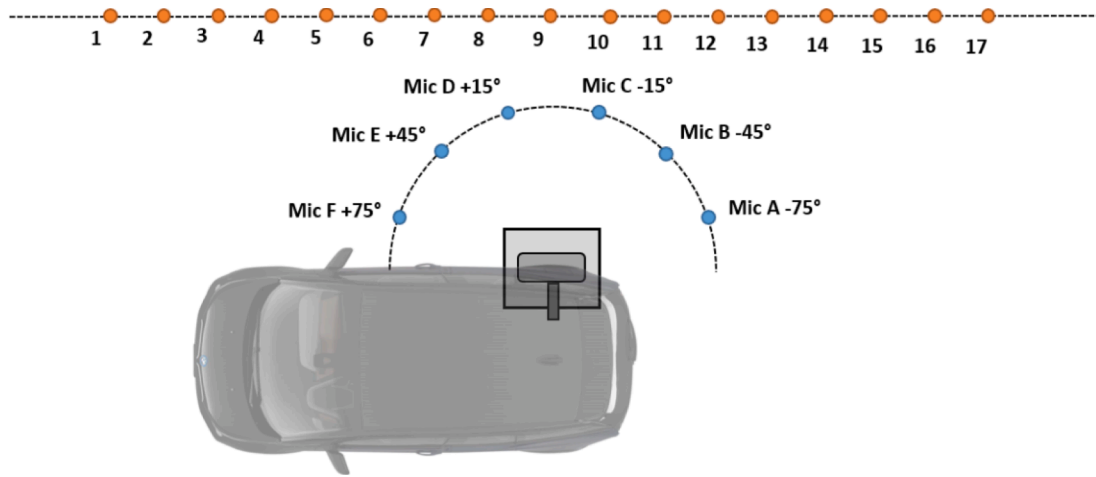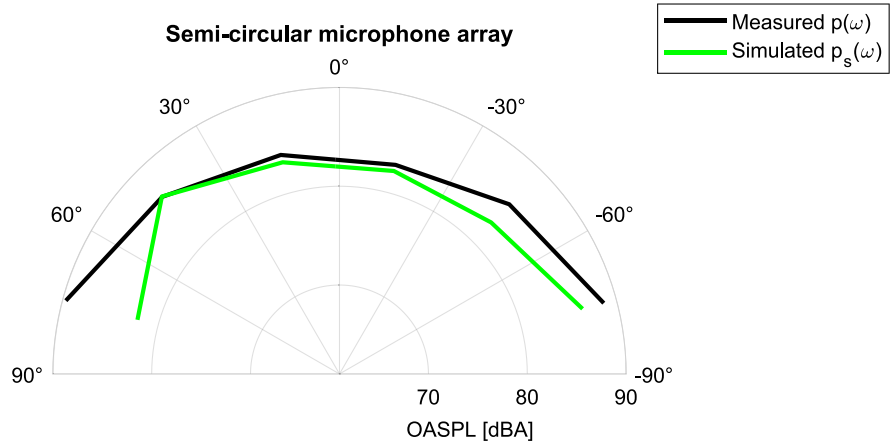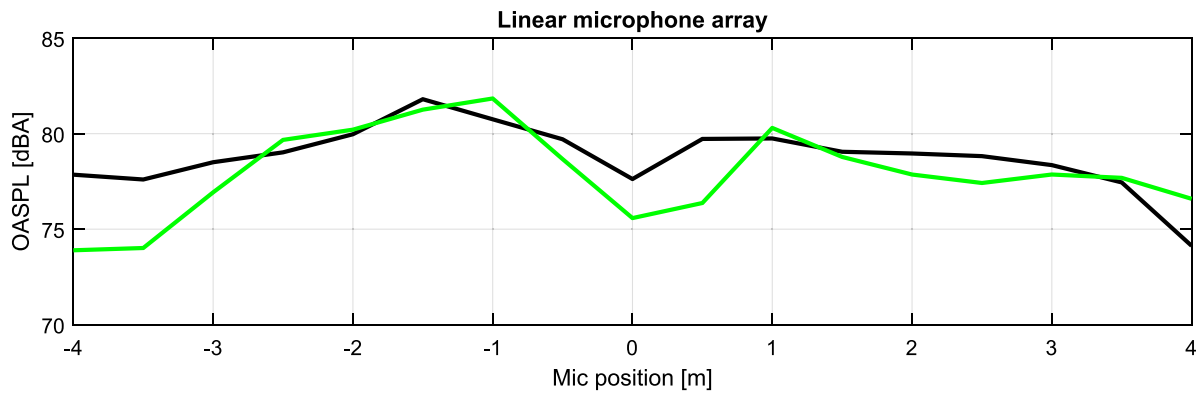
(a)

(b)

Fig. 11. In (a), the experimental setup for the front right tyre test. In (b), a comparison of the OASPLs between the measured deterministic noise component (in black) and that simulated (in green).

(a)

(b)

Fig. 12. In (a), the experimental setup for the rear right tyre test. In (b), a comparison of the OASPLs between the measured deterministic noise component (in black) and that simulated (in green).

Declaration of Competing Interest

The authors declare that they have no known competing financial interests or personal relationships that could have appeared to influence the work reported in this paper.

Data availability

The data that has been used is confidential.

Acknowledgements

References

[1] European Environment Agency. Environmental noise in Europe - 2020. Luxemburg: 2020.

[2] Sandberg U. Tyre/road noise : myths and realities. 2001 International Congress and Exhibition on Noise Control Engineering. 2001.

[3] ISO 13325:2019 Tyres — Coast-by methods for measurement of tyre-to-road sound emission. 2019.

[4] ISO 362-1:2022 Acoustics — Engineering method for measurement of noise emitted by accelerating road vehicles — Part 1: M and N categories. 2022.

[5] ISO 10844:2021 Acoustics — Specification of test tracks for measuring sound emitted by road vehicles and their tyres. 2021.

[6] REGULATION (EC) No 661/2009 OF THE EUROPEAN PARLIAMENT AND OF THE COUNCIL. 2009.

[7] ISO 362-3:2022 Acoustics — Measurement of noise emitted by accelerating road vehicles — Engineering method — Part 3: Indoor testing M and N categories. 2022.

[8] Li T, Burdisso R, Sandu C. Literature review of models on tire-pavement interaction noise. J Sound Vib 2018;420:357–445. https://doi.org/10.1016/j.jsv.2018.01.026.

[9] Mohammadi S, Ohadi A, Irannejad-Parizi M. A comprehensive study on statistical prediction and reduction of tire/road noise. J Vib Control 2022;28:2487–501. https://doi.org/10.1177/10775463211013184.

[10] Rapino L, Liu L, Dinosio A, Ripamonti F, Corradi R, Baro S. Processing of tyre data for rolling noise prediction through a statistical modelling approach. Mech Syst Signal Process 2023;188:110042. https://doi.org/10.1016/j.ymssp.2022.110042.

[11] Lee S-K, Lee H, Back J, An K, Yoon Y, Yum K, et al. Prediction of tire pattern noise in early design stage based on convolutional neural network. Appl Acoust 2021; 172:107617. https://doi.org/10.1016/j.apacoust.2020.107617.

[12] Brinkmeier M, Nackenhorst U, Petersen S, von Estorff O. A finite element approach for the simulation of tire rolling noise. J Sound Vib 2008;309:20–39. https://doi.org/10.1016/j.jsv.2006.11.040.

[13] Banz L, Gimperlein H, Nezhi Z, Stephan EP. Time domain BEM for sound radiation of tires. Comput Mech 2016;58:45–57. https://doi.org/10.1007/s00466-016-1281-3.

[14] Sandberg U, Tyre EJA, road,. Noise Reference Book INFORMEX 2002.

[15] Wang X. Automotive Tire Noise and Vibrations. Elsevier 2020. https://doi.org/10.1016/C2018-0-02431-7.

[16] Sandberg U, Ejsmont JA. Tire/Road Noise—Generation, Measurement, and Abatement. Handbook of Noise and Vibration Control, Hoboken, NJ, USA: John Wiley & Sons, Inc.; n.d., p. 1054–71. https://doi.org/10.1002/9780470209707.ch86.

[17] Hoever C, Tsotras A, Pallas M-A, Cesbron J. Factors influencing tyre/road noise under torque. Internoise 2022–51st International Congress and Exposition on Noise Control Engineering. 2022.

[18] Liao G, Sakhaeifar MS, Heitzman M, West R, Waller B, Wang S, et al. The effects of pavement surface characteristics on tire/pavement noise. Appl Acoust 2014;76: 14–23. https://doi.org/10.1016/j.apacoust.2013.07.012.

[19] Bravo T. An analytical study on the amplification of the tyre rolling noise due to the horn effect. Appl Acoust 2017;123:85–92. https://doi.org/10.1016/j.apacoust.2017.03.009.

[20] Ejsmont JA, Sandberg U, Taryma S. Influence of Tread Pattern on Tire/Road Noise. SAE Trans 1984;93:632–40.

[21] Feng J, Sandu C, Li T, Burdisso R. The Effects of Tread Pattern on Tire Pavement Interaction Noise. INTER-NOISE 2016, 2016..

[22] Nelson PA, Yoon SH. Estimation of acoustic source strength by inverse methods: Part I, conditioning of the inverse problem. J Sound Vib 2000;233:639–64. https://doi.org/10.1006/jsvi.1999.2837.

[23] Yoon SH, Nelson PA. Estimation of acoustic source strength by inverse methods: Part II, experimental investigation of methods for choosing regularization parameters. J Sound Vib 2000;233:665–701. https://doi.org/10.1006/jsvi.2000.2836.

[24] Bobrovnitskii YI, Pavic G. Modelling and characterization of airborne noise sources. J Sound Vib 2003;261:527–55. https://doi.org/10.1016/S0022-460X(02)00981-1.

[25] Lafont T, Stelzer R, D'Amico R, Kropp W, Bertolini C. Modelling tyre noise in finite element simulations for pass-by noise predictions. Proc Inst Mech Eng C J Mech Eng Sci 2019;233:6398–408. https://doi.org/10.1177/0954406219832908.

[26] Bécot F-X. Tyre noise over impedance surfaces - Efficient application of the Equivalent Sources method. 2003.

[27] Berckmans D, Kindt P, Sas P, Desmet W. Evaluation of substitution monopole models for tire noise sound synthesis. Mech Syst Signal Process 2010;24:240–55. https://doi.org/10.1016/j.ymssp.2009.06.005.

[28] Li Q, Ripamonti F, Corradi R, Caccialanza M. Simulation of deterministic tyre noise based on a monopole substitution model. Appl Acoust 2021;178. https://doi.org/10.1016/j.apacoust.2021.108009.

[29] Li T. A state-of-the-art review of measurement techniques on tire–pavement interaction noise. Measurement 2018;128:325–51. https://doi.org/10.1016/j.measurement.2018.06.056.

[30] Mioduszewski P, Berge T. Tyre/road noise measurements on ISO tracks using the modified CPX method. In: Internoise 2022–51st International Congress and Exposition on Noise Control Engineering; 2022. https://doi.org/10.3397/IN_2022_0375.

[31] Nowak J, Wehr R, Haider M, Kaltenbacher M. Inverse scheme for sound source identification in a vehicle trailer. Internoise 2022–51st International Congress and Exposition on Noise Control Engineering. 2022.

[32] Corradi R, Ripamonti F, di Lione R, Caccialanza M. Test methodologies for mapping tyre exterior noise in semi-anechoic chamber. INTER-NOISE 2019, 2019..